Chapter 4

Chaotic, Stochastic Resonance, and Anti-Resonance Phenomena in Optics

Vladimir L. Kalashnikov

Additional information is available at the end of the chapter

http://dx.doi.org/10.5772/intechopen.70737

Abstract

Existence of different, frequently incommensurate scales is a common phenomenon in nature. Interactions between processes characterized by different scales can result in a multitude of emergent phenomena when a system cannot be described as a scale-separated hierarchy of underlying processes but presents a substantially new entity with qualitatively new properties and behavior. Striking examples are life, fractals, and chaos. Here, we shall demonstrate the quite nontrivial phenomena: chaotic and stochastic resonances and anti-resonance on examples of laser systems. The phenomena of resonant stochastization (stochastic anti-resonance), self-ordering (stochastic resonance), and resonant chaotization of coherent structures (dissipative solitons) are considered on the examples of mode-locked lasers and Raman fiber amplifiers. Despite a well-known effect of noise suppression and global regularization of dynamics due to the resonant interaction of noise and regular external periodic perturbation, here we report about the reverse situation when the regular and noise-like perturbations result in the emergent phenomena ranging from the coherent structure formation to the fine-grained chaotic/noisy dynamics. We guess that the nonlinear optical systems can be considered in this context as an ideal test-bed for "metaphorical modeling" in the area of deterministic and stochastic dynamics of resonance systems.

Keywords: chaotic and stochastic resonance/anti-resonance, soliton-emergence phenomena, resonant soliton–linear wave interaction, noise-assisted coherence, "metaphorical" optical modeling, resonance vector mode-locking

1. Introduction

Is a noise so destructive? This question is not only philosophical because it is directly addressable. We live in a noisy environment, and who knows, would such environment be extremely constructive, namely constructive? Why not? For instance, the growth of initial quantum

gravitational perturbations gives birth to our Universe as a quite-ordered structure, and our brains are very flowing but constructive, isn't that so? The key point is a resonant interaction of noise with a *nonlinear* system [1, 2]. The resonance phenomena in nonlinear systems are fraught with counterintuitive consequences. Noise can enhance a system's internal coherence [*stochastic resonance*, (SR)] or damage it [*stochastic anti-resonance*, (SAR)]. Both effects are resonantly sensible to the system parameters that allow naming both phenomena as *a resonance* with taking into account a principal difference between the *linear* and *nonlinear* systems far from an equilibrium state [3].

The notion of SR occurred unexpectedly from the studies regarding the long-term climatic changes (i.e., the ice ages) when the short-term (1-year scaled) climatic noise enhances resonantly an incommensurable weak variation (~10^5 years) of the Earth ecliptic [4, 5]. The excellent surveys expose a further progress forwarding this direction [3, 6–11]. A development of the SR ideology in the fields of neuroscience, biology, and information processes was especially exciting. A noise-induced resonant enhancement of neural sensibility, adaptivity, and learning capability was demonstrated and analyzed [10, 12–18].

The classical theory of SR was based on the resonant transitions in noisy bi-stable nonlinear systems [19–21]. Further studies revealed that both SR and SAR cover an extremely broad range of phenomena including escape from the metastable state, threshold "firing" dynamics, dynamics assisted by deterministic chaos, regularization induced by coherent periodic or continuous structures without a noise assistance, etc [3, 22, 23]. Therefore, the terms of SR and SAR can be misleading in some respects, and it is better to speak about a broad range of phenomena in the nonlinear systems far from equilibrium, which is caused by the resonant-like interaction between processes with incommensurable characteristic scales [3, 24].

As a classical illustration of SR, one may consider the so-called FitzHugh-Nagumo (FN) model (e.g., see [3] and references ibidem), which describes a noise excitable evolution in a very simple two-dimensional form:

$$\epsilon \frac{dx}{dt} = f(x) - y, \quad \frac{dy}{dt} = \gamma x - \beta y - s(t) + \sqrt{2D}\zeta(t), \tag{1}$$

where a potential function is defined as $f(t) = x - ax^3$, typically ϵ defines a ratio of evolutional scales between x and y variables, γ is a coupling parameter, β is a friction coefficient, and $s(t)$ is a periodic external force ($s(t) = \alpha \cos[\omega t]$, usually). The last term in Eq. (1) describes a Wiener stochastic process with volatility $2D$. The stochastic Eq. (1) is treated in the Stratonovich's sense. Evolution of dynamical variables in the absence of noise and periodic modulation is shown in **Figure 1**, which demonstrates a relaxation to local minimum of potential.

Separated effects of small harmonic modulation and noise are shown in **Figure 2**. One can see that they have a "perturbative" character and induce the small oscillations/fluctuations around the potential local minimum.

http://dx.doi.org/10.5772/intechopen.70737

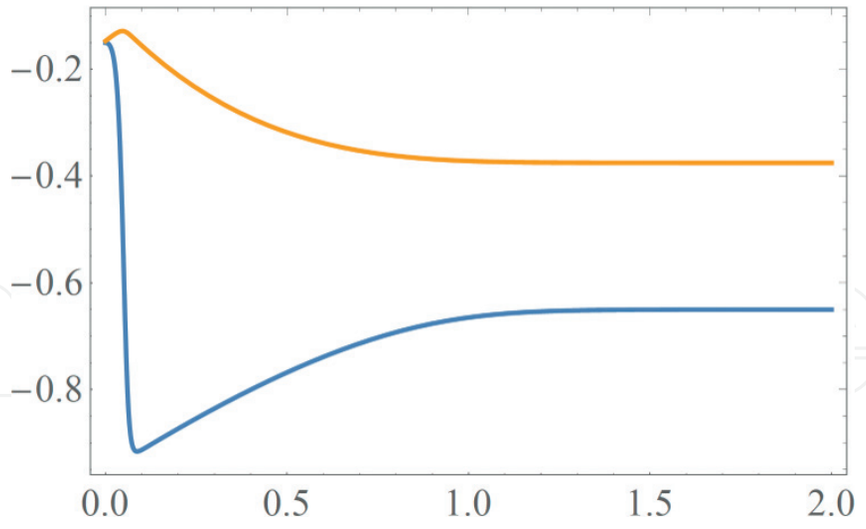

Figure 1. Evolution of $x(t)$ (the lower curve) and $y(t)$ (the upper curve) in the absence of stochastic and modulation terms in Eq. (1) (i.e., $(D, \alpha)=0$) within the range of $t \in [0, 2]$. $\epsilon=0.01$, $a=1$, $b=0.6$, $\beta=1$, $\gamma=1.5$.

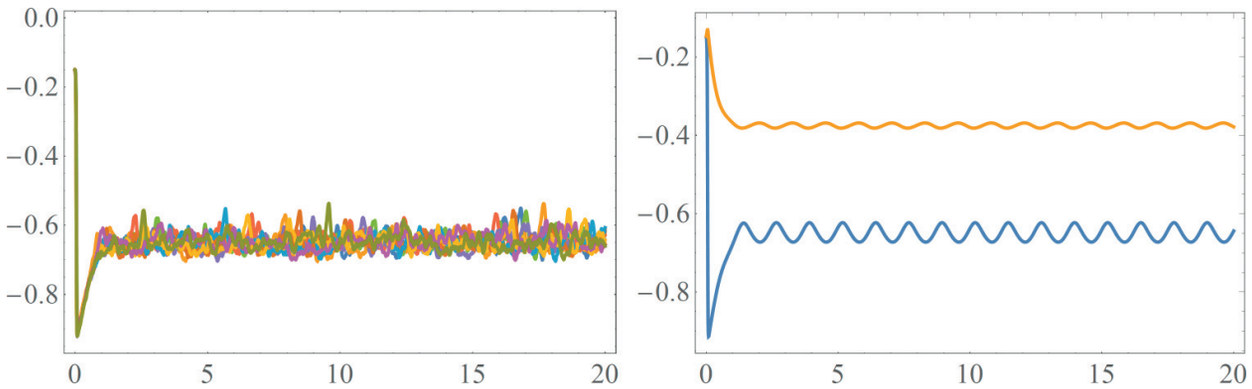

Figure 2. Left: Evolution of $x(t)$ (the lower curve) and $y(t)$ (the upper curve) in the absence of stochastic and presence of modulation terms in Eq. (1); $\alpha=0.05$ and $\omega=5$. Right: Ten stochastic trajectories for $x(t)$ in the absence of harmonic modulation; $D=0.01$. Other parameters correspond to **Figure 1**.

However, the situation changes drastically under the common action of noise and external modulation (**Figure 3**). Extremal and almost regular spikes appear at a frequency, which is lower than the modulational one and incommensurable with the noise scale. One may consider this example based on the FN-model as an impressive and quite simple illustration of SR.

At this moment, there is a huge amount of work concerning the SR and SAR as well as their variations and modifications. We refer a reader to the above-cited books and surveys (the reference list is not exhaustive, of course). A spectacular demonstration of SR in a ring dye laser [25] gave impetus to an intensive exploration of this field. Therefore, we intend to discuss some aspects of SR, SAR, coherent resonant, and multi-scale phenomena regarding laser optics and solitonics.

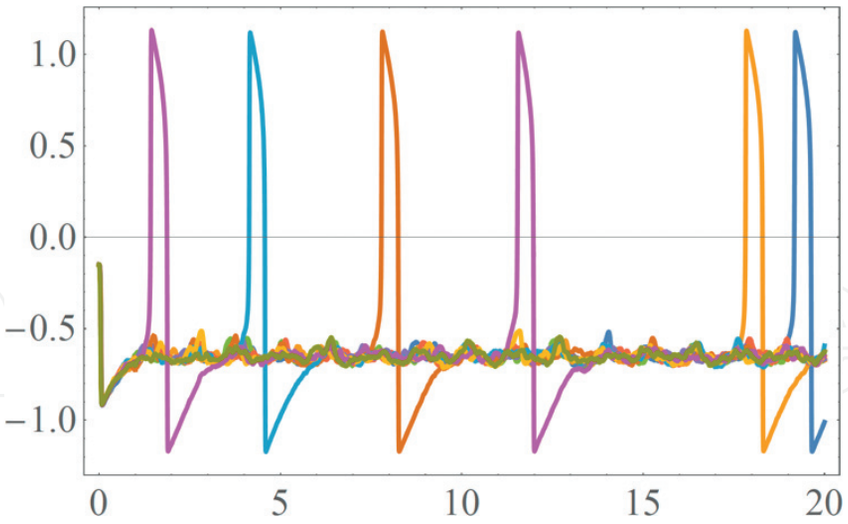

Figure 3. SR appearing under joined action of factors illustrated in **Figure 2**.

This paper is organized as follows. In the next section, we expose the SAR phenomenon in a Raman fiber amplifier. Then, the chaotic resonance of dissipative soliton with linear waves will be considered. Further, the SR and SAR as well as multi-scale resonant phenomena in mode-locked lasers will be exposed. Finally, the resonance vector mode-locking will be described in a nutshell.

2. SAR in a Raman fiber amplifier

A Raman amplifier can be considered as a test-bed for the study of SAR and multi-scale dynamics due to a comparative simplicity and realizability and, simultaneously, high practical significance. The latter is defined by the fact that Raman amplification provides an efficient tool for optical telecommunication lines with frequency multiplexing (for details see [26]). In such lines, there are very different scales: a length corresponding to the width of pulse carrying information (~10 – 100 mm), commensurable lengths of polarization beats and inherent stochastic distortions of a fiber (~10 – 100 m), attenuation length (~10 km), nonlinear and dispersion lengths (>100 km), and overall propagation length (>10^7 m) [27].

The Raman amplification is sensitive to the relative polarization of gain and signal—a gain is maximum for copolarized pump and signal but minimum for their mutually transverse polarizations. Since beat rates for signal (b_s) and pump (b_p) differ, it causes a periodical modulation of the Raman gain with fiber length [26]. Simultaneously, the polarization properties (birefringence) of fiber are sensitive to the inevitable *stochastic* breakdowns of the fiber cylindrical symmetry [27]. Thus, one has all necessary prerequisites for the manifestation of SR and SAR phenomena.

The extended vector theory of the stimulated Raman scattering with taking into account the random birefringence is presented in [26–28]. The system of stochastic differential equations

http://dx.doi.org/10.5772/intechopen.70737

describing an evolution of copropagating pump and signal states of polarization (SOP) under the action of random fiber birefringence can be written in the following form [27]:

$$\frac{d\vec{S}}{dz} = \frac{g_R}{2}\left(\left|\vec{P}\right|\vec{S} + \left|\vec{S}\right|\vec{P}\right) - \alpha_s\,\vec{S} + \beta\begin{pmatrix} S_2 \\ -S_1 \\ 0 \end{pmatrix} + 2b_s\begin{pmatrix} 0 \\ -S_3 \\ S_2 \end{pmatrix}, \tag{2a}$$

$$\frac{d\vec{P}}{dz} = -\frac{\omega_p}{\omega_s}\frac{g_R}{2}\left(\left|\vec{P}\right|\vec{S} + \left|\vec{S}\right|\vec{P}\right) - \alpha_p\,\vec{P} + \beta\begin{pmatrix} P_2 \\ -P_1 \\ 0 \end{pmatrix} + 2b_p\begin{pmatrix} 0 \\ -P_3 \\ P_2 \end{pmatrix}, \tag{2b}$$

where $\vec{S} = S_0\,\vec{s}$ and $\vec{P} = P_0\vec{p}$ are the projections of signal and pump powers with the corresponding unit vectors $\vec{s}$ and $\vec{p}$ ($S_0 = \left|\vec{S}\right|$, $P_0 = \left|\vec{P}\right|$) in the Stokes representation. The Raman gain coefficient is g_R, and the pump/signal frequencies are $\omega_{p,s}$, respectively. The attenuation constants for the pump and signal are $\alpha_{p,s}$. The most interesting parameters are $b_{p,s} = 2\pi/L_{p,s}$ ($L_{p,s}$ are the pump/signal beat lengths, respectively) and the Wiener *stochastic* term with the zero drift and the volatility $\sigma^2 = 1/L_c$: $\langle\beta(z), \beta(z')\rangle = \sigma^2\delta(z - z')$ (L_c is a correlation length of the stochastic material birefringence).

The variation of L_c (correlation length defining a noise "strength") relatively $L_{p,s}$ (periods of the deterministic polarization beatings) causes a transition between the different regimes.

i. A strong polarization pump/signal coupling (**Figure 4**, left) corresponds to a case of $L_{p,s} \gg L_c$ when a noise is too "fine-grained" and cannot distort nonlinear trapping of signal by pump. As a result, the mutual polarizations of pump and signal are highly correlated, and the signal fluctuations are small (≈1% in the case under consideration; see **Figure 5**, left).

ii. When $L_{p,s}$ approach L_c (i.e., relative strength of noise increases), the signal and pump decouple (**Figure 4**, middle), and the signal evolution becomes extremely noisy (**Figure 5**, middle).

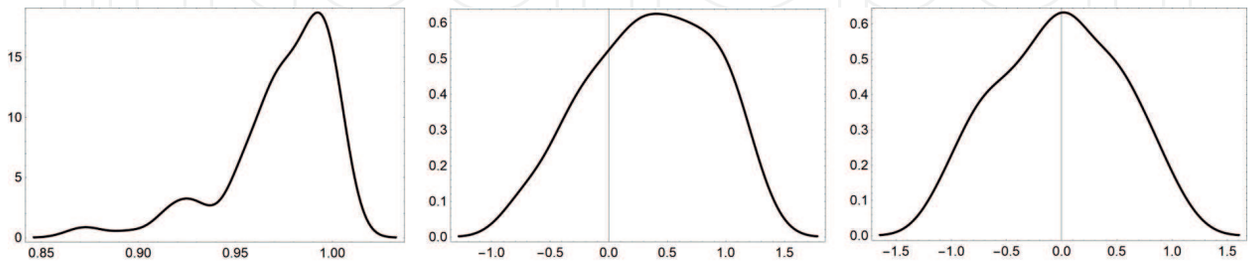

Figure 4. PDF of the normalized output signal-pump scalar product $\vec{S}\vec{P}/\left|\vec{S}\right|\left|\vec{P}\right|$ with lowering beat lengths $L_{p,s}$ [29]. $L_c = 100$ m, $L_s = 1$ km (left), 150 m (middle), 30 m (right); $L_p = 1.55L_s/1.465$ (an Er-doped fiber), the propagation length $L = 5$ km. The input powers of pump and signal are 1 and 0.01 W, respectively.

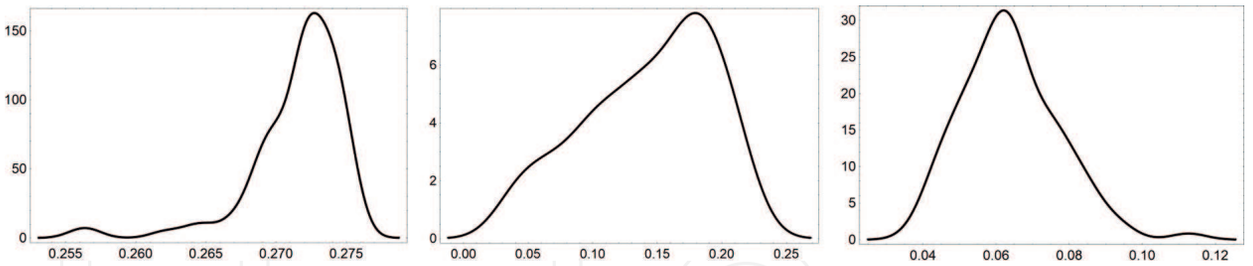

Figure 5. PDF of the output signal power $\left|\vec{S}\right|^2$ (in Watts) with lowering beat lengths $L_{p,s}$ as in **Figure 4** [29].

iii. Further decrease of $L_{p,s}$ relatively L_c causes almost complete decoupling of pump and signal (so-called diffusion limit; **Figure 4**, right) when a fiber behaves like an isotropic medium. Noise plays important but diminishing role (**Figure 5**, right).

Such a resonant-like enhancement of irregularity that depends on the relative strengths of noise and regular oscillations is an example of SAR. **Figure 6** is a spectacular illustration of this phenomenon based on the model of Eqs. (2a) and (2b) [30]. We can see here the resonant enhancement of a Raman gain standard deviation defined as $\sigma_G = \sqrt{\left|\vec{S}(L)\right|^2 \Big/ \left|\vec{S}(L)\right|^2 - 1}$ in dependence on a fiber length L and a polarization mode-dispersion parameter $D_p = 2\lambda_s\sqrt{L_c}/cL_s$ defining relative contribution of stochastic and deterministic polarization effects (λ_s and c are the signal wavelength and the speed of light, respectively).

The phenomenon of SAR can be explained as an escape from a metastable state corresponding to pump-signal pulling with an effective potential barrier ΔU and an "intra-well relaxation time"

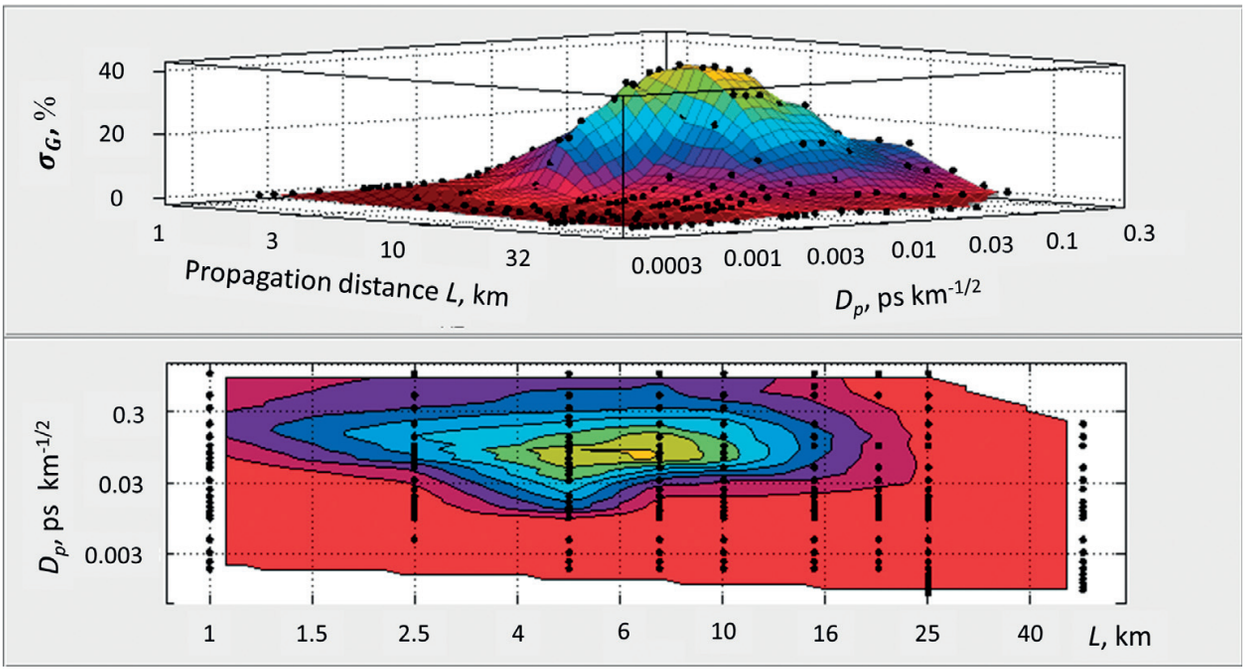

Figure 6. Relative standard deviation of the maximum Raman gain coefficient illustrating the SAR in a fiber Raman amplifier [30].

http://dx.doi.org/10.5772/intechopen.70737

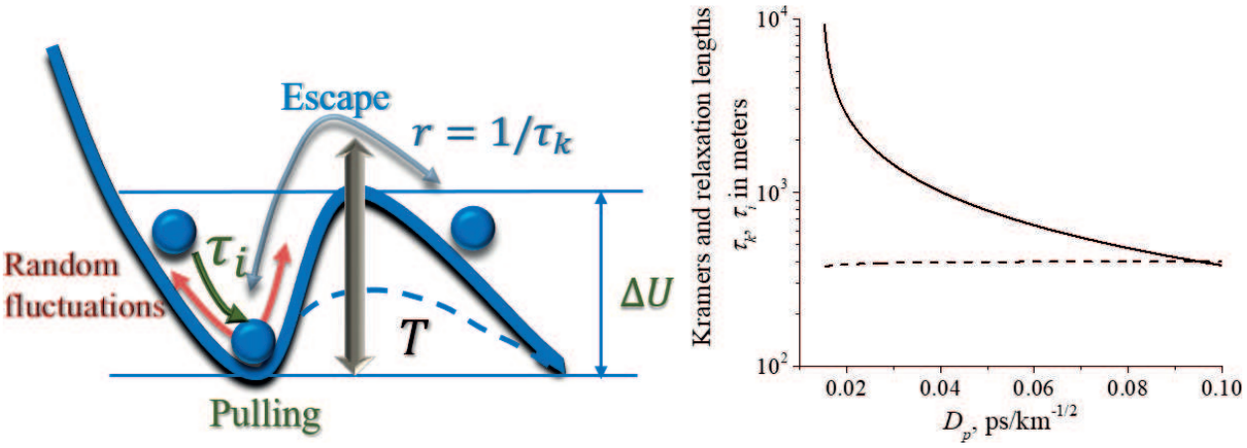

Figure 7. Left: Noise causes an escape from metastable (polarization pulling) state through a potential barrier ΔU controlled by periodic modulation T induced by regular polarization beating. Right: Dependence of Kramers length τ_k (solid curve) and intra-well relaxation length τ_i (dashed curve) on the polarization mode-dispersion parameter D_p [27, 31].

(or length in our case) τ_i (**Figure 7**, left) [27, 31]. The random fluctuations can cause an escape from this metastable state with an escape rate $r \propto \exp\left(-\frac{\Delta U}{D}\right) = 1/\tau_k$ defined by the so-called *Kramers time* (*length*) τ_k (D is an effective "temperature" defining a noise strength) [6, 32]. The periodic (T) modulation of potential barrier caused by the polarization beatings can enlarge this effective temperature and, thereby, increase the escape rate (**Figure 7**, right) [27, 31].

Thus, a Raman fiber amplifier can be considered as a simple and practically valuable test-bed for a demonstration of SAR that is a phenomenon of noise-induced escape from the metastable state. Practical control of this phenomenon is especially important for the development of modern high-speed optical communication lines that promise to exceed the limits of existing broadband information infrastructure.

3. Chaotic resonance between a dissipative soliton and linear waves

Dissipative soliton (DS) is a well-localized structure self-emergent in dissipative systems. Such structures appear in different areas ranging from physics to biology, medicine, and even economy and sociology [33, 34]. The simplest equation regarding the DS modeling is the so-called generalized complex nonlinear Ginzburg-Landau equation (CNGLE) [33–35]:

$$\frac{\partial A(z,t)}{\partial z} = \left\{-\sigma + \alpha\frac{\partial^2}{\partial t^2} + \left[\kappa\left(1 - \zeta|A(z,t)|^2\right)|A(z,t)|^2\right]\right\}A(z,t) + i\left\{\frac{\beta_2}{2}\frac{\partial^2}{\partial t^2} - \gamma|A(z,t)|^2\right\}A(z,t) + \frac{\beta_3}{6}\frac{\partial^3}{\partial t^3}A(z,t) + s(t), \tag{3}$$

where a field of amplitude A, slowly-varying with a local time t, propagates along a coordinate z under action of dissipative (first braces) and nondissipative (second braces) factors. Then,

σ-parameter corresponds to energy-dependent net-loss, α-parameter defines spectral losses, κ- and ζ-parameters describe effective nonlinear gain and its depletion, respectively. Nondissipative factors are self-phase modulation (SPM, γ), group-delay dispersion (GDD, β_2) with low-order correction to the latter (third-order dispersion or TOD, β_3). $s(t)$ describes a complex white noise.

The general-form of DS solutions of Eq. (3) is unknown, and the extensive numerical simulations are required to investigate the complexity of DS dynamics. However, there are some very simple considerations based on resonance/balance relations, which allow understanding some basic properties of DS.

Indeed, a steady-state solution of Eq. (3) has a form $A(t,z)=E(t)\exp(-iqz)$, where the soliton wave number q is related to the carrier-envelope offset [36], which results from nonlinear phase shift caused by SPM: $q=\gamma P_0$ (P_0 is a DS peak power) [37]. The dispersion relation for linear waves is $k(\omega)=\beta_2\omega^2/2$. Hence, to be stable (i.e., nonradiating), the DS spectrum has to be truncated at the frequencies $\pm\Delta$: $k(\pm\Delta)=q$, where $\Delta=\sqrt{2\gamma P_0/\beta_2}$ (**Figure 8**) [35].

Simultaneously, the spectral loss $\sim\alpha\Delta^2$ has to be compensated by the nonlinear gain $\sim\kappa P_0$. This condition plus the resonant condition give the rough stability criterion for DS:

$$\alpha\gamma/\kappa\beta_2 \le 1/2, \tag{4}$$

which interrelates dissipative and nondissipative factors contributing to DS formation (more precise analysis can be found in [38]).

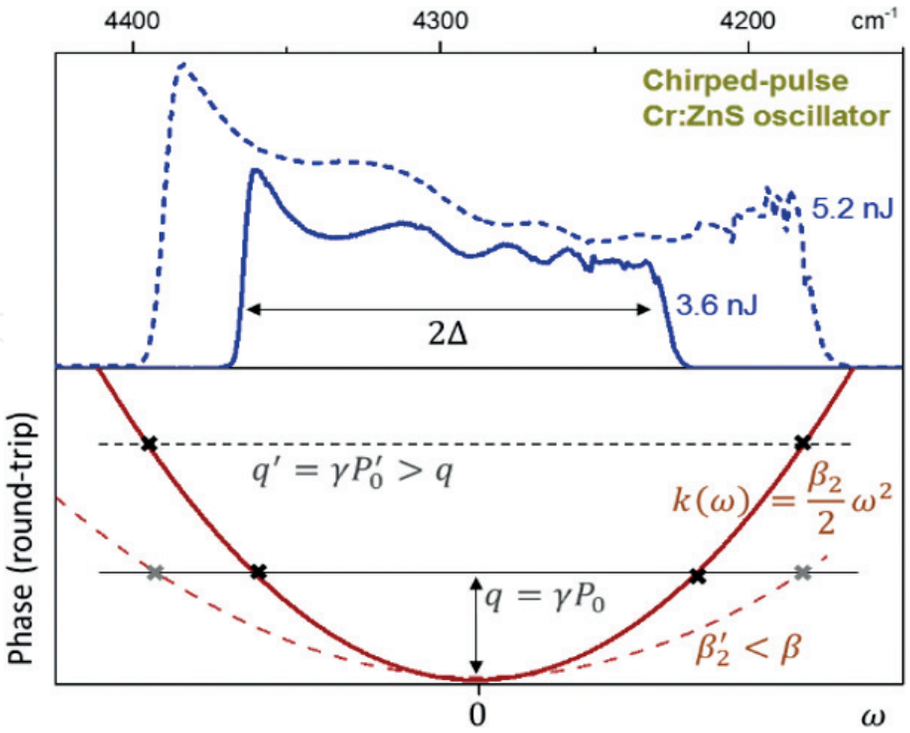

Figure 8. *Resonance condition* (black and gray crosses at the bottom panel) for the DS defines the spectrum width 2Δ. Changing the power and/or the dispersion (solid and dashed lines in the bottom panel) controls the spectrum width. Lines in the top panel show the experimental spectra corresponding to different energies [35].

TOD modifies the dispersion condition for a linear wave so that the resonant condition becomes: $q = \frac{\beta_2\omega^2}{2} + \frac{\beta_3\omega^3}{6}$ (black/red online/curve in **Figure 9c**). It can cause an appearance of additional resonant frequency which proximity to DS spectrum (i.e., to one of the other resonant frequencies) can initiate chaotic dynamics [39, 40]. This conjecture was confirmed in [35] both experimentally and numerically.

Figure 9 demonstrates an example of such chaotization obtained from numerical simulations of Eq. (3) (for details, see [35]). The Wigner function (time-frequency diagram, **Figure 9a**) consists of strongly distorted DS-part near 2.3 μm (dark-red region online) and long dispersive tale in spectral domain around 2.4 μm (yellow – light blue region online), which co-propagates with DS and, as an analysis shows, collides with it in time domain. As a result, the DS spectrum becomes modulated chaotically (**Figure 9b**), but the averaged spectrum looks quite smooth with the characteristic shape of "*Boa constrictor* digesting an elephant" (**Figure 9d**) [35]. As was mentioned, these phenomena can be explained as a nonlinear resonance of three-coupled oscillators [41, 42] when the TOD-induced resonant point (DW in **Figure 9c**) approaches one of the other two (R_2, in our case).

The last statement can be confirmed by a reconstruction of phase space corresponding to the chaotic dynamics in **Figure 9**. Such a reconstruction is based on the standard lag-delayed procedure when one tries to reconstruct an N-dimensional phase space from time-series data $V(t)$ by the means of following discretization: $[V(t), V(t+L), V(t+2L), \ldots, V(t+(N-1)L)]$, where L is a time-lag [43]. As a rule, an appropriative time-lag is defined from the first zero of autocorrelation function of time-series (peak powers in our case). The corresponding reconstruction is shown in **Figure 10** [35]. One can see, that the chaotic trajectory of $P_0(t)$ is

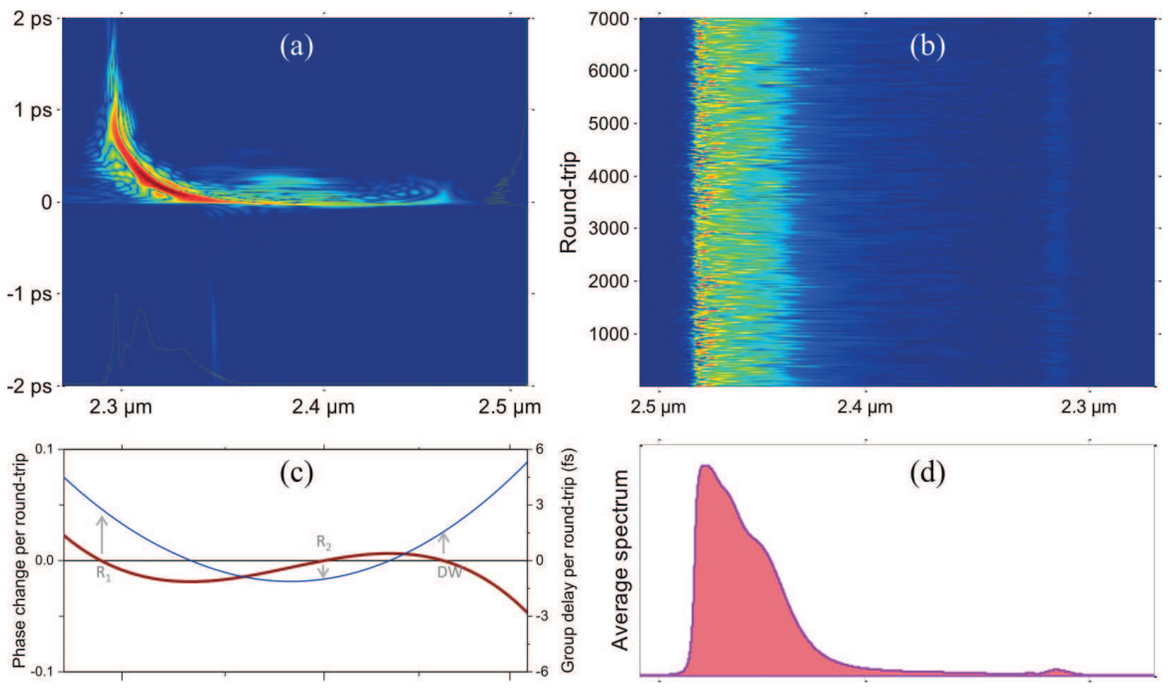

Figure 9. Chaotization of DS dynamics due to resonant interaction with a linear wave in the presence of TOD. (a) Single-shot Wigner function (time-frequency diagram) of DS. (b) Spectra of DS over the 7000 laser cavity round-trips. (c) Round-trip phase (gray) and group delays (black, red online). (d) Accumulated spectrum [35].

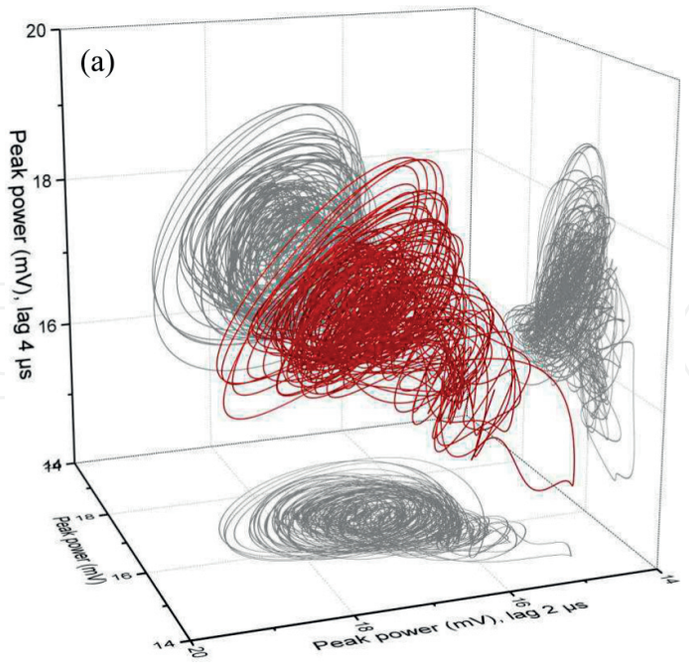

Figure 10. Phase space reconstructed from the experimental DS peak power set [35].

completely embedded in the three-dimensional manifold, and the attracting manifold has a typical toroidal shape. Both facts validate a model of nonlinear resonance of three coupled oscillators.

4. Stochastic resonance and anti-resonance in mode-locked lasers

A laser, as a device locking electromagnetic waves, possesses a discrete set of longitudinal modes, i.e., set of standing waves, which interacts irregularly due to random mutual phases. Locking of a mutual phase between modes, namely mode-locking, results in the generation of a high-intensive ultra-short laser pulse circulating with the repetition rate multiple of the period of laser resonator (e.g., see [44, 45]). In the time domain, the ultra-short pulse formation can be described in the frameworks of the so-called *fluctuation model* [46, 47], which treats a pulse[1] emerging as a process of amplification and selection of noise fluctuations (see **Figure 11**). Such a model demonstrates a crucial role of noise in ultra-short pulse dynamics. The noise is not only a source of pulse formation, but it can also affect the pulse dynamics at all stages. In particular, it is a source of "linear" (dispersive) waves, which can resonantly interact with a pulse and randomize its dynamics (see the previous section).

The typical equation with "distributed" laser parameters is Eq. (3). It describes a multitude of realistic phenomena intrinsic to the pulse dynamics. But in many real-world situations, the "discretized" models are more relevant. For instance, let us consider a system of laser

[1]We use the term "pulse" instead of DS because it is more appropriate to "discretized" systems for which the notion "soliton" can be misleading.

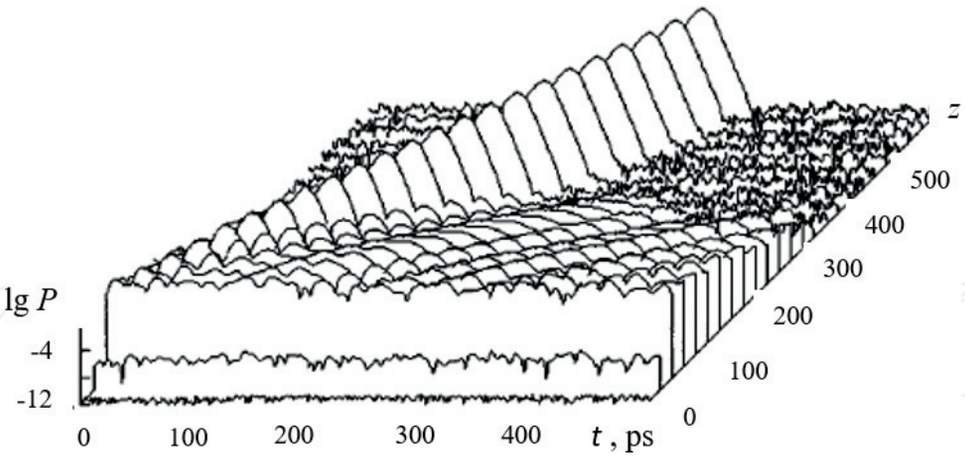

Figure 11. Formation of the ultra-short pulse from initial noise fluctuations (P is a normalized power, t is a local time, z is a cavity round-trip number) [48]. Noise is suppressed on the final stage, but remains on a "vacuum level.".

resonantly coupled with an external resonator. In the dispersion-less case, the field evolution in a laser can be described as follows [49]:

$$\begin{aligned} A'(z,t) &= A(z,t)\exp\left[g(t) - i\gamma|A(z,t)|^2\right] + s(t), \\ \frac{\partial g(t)}{\partial t} &= \sigma_{14}\left(g_m - g(t)\right)I_p/h\nu_p - \sigma_{32}g(t)|A(z,t)|^2/h\nu - \frac{g(t)}{T_{31}}. \end{aligned} \tag{5}$$

Here, both z and t are discretised so that z is a cavity transit number, and t is a local time discretised with a step Δt. The coefficient $g(t)$ describes a local gain for a 4-level active medium with the maximal gain g_m for full population inversion: σ_{14}, σ_{32}, and T_{31} are absorption, emission cross-section, and gain relaxation time, respectively. ν_p and ν are pump and generation wavelength, respectively.

$$s(t) = s(t - \Delta t)\exp\left[-\frac{\Delta t}{t_{coh}}\right] + s_0\exp\left[i\phi(t)\right], \tag{6}$$

is a noise term with the coherence time t_{coh}, a noise level s_0, and a random phase $\varphi(t)$ [50].

Spectral dissipation is provided by a Fabry-Pérot etalon with a group-delay t_f [51]:

$$A''(z,t) = \left(1 - R_f\right)A'(z,t) + R_f A''(z, t - \Delta t), \tag{7}$$

where $R_f = t_f/(t_f + \Delta t)$.

The field A is coupled with the field in external resonator $B(z, t)$ [49]:

$$\begin{aligned} A(z+1,t) &= RA''(z,t) - i\theta T\exp\left[i\pi\phi\right]B(z,t), \\ B(z+1,t) &= -i\theta TA''(z,t) + \theta^2 R\exp\left[i\pi\phi\right]B(z,t), \end{aligned} \tag{8}$$

where R, T, and θ are reflection, transmission, and coupling coefficients, respectively.

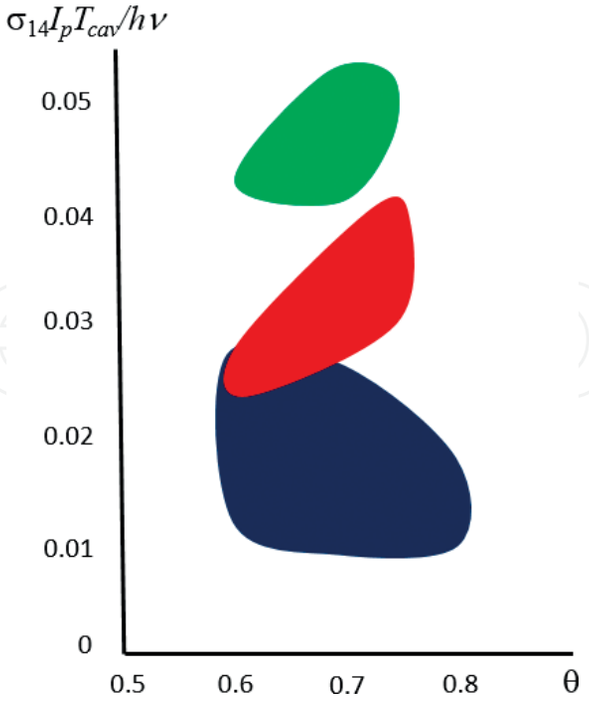

Figure 12. Regions of mode-locking self-start for the model (5–8). $\gamma h\nu/\sigma_{32}T_{cav}=0.01$, $\varphi=0$, $t_f=1$ ps, $t_{cor}=\infty$ (bottom region), 1 μs (middle region), and 1 ps (top region). T_{cav} is a cavity period.

It is interesting to consider the question about disruptiveness of noise for pulse formation. **Figure 12** shows the regions of formation of stable pulses from noise (so-called regions of mode-locking self-start) for different t_{coh}. One can see, that the decrease of noise coherence is destructive from the points of view of the mode-locking regions size and the threshold pump intensity providing mode-locking.

However, the simulations demonstrate that even very low-frequency external modulation (e.g., by moving resonator mirror inducing the Doppler shift of optical wave) can suppress noise (see **Figure 13**) and stabilize dynamics [52, 53]. This phenomenon can be interpreted as a manifestation of resonant interaction of scale-incommensurable processes. Moreover, exactly such a resonance provides mode-locking self-start in the majority of lasers (moving mirror technique [54] or even simple mirror knocking).

In close connection with the phenomenon mentioned above, one has to note that a nonlinear interconnection between the scale-incommensurate processes is a crucial factor defining all considered phenomena. An interesting example closely connected with previous one is a laser mode-locked by external phase modulation [55, 56]. This system can be described by following equation (compare with Eq. (3)):

$$\frac{\partial A(z,t)}{\partial z}=\left\{-\sigma-\delta\frac{\partial}{\partial t}+\alpha\frac{\partial^2}{\partial t^2}-i\gamma|A(z,t)|^2\right\}A(z,t)+i\omega tA(z,t), \tag{9}$$

where $-\sigma$ is a saturated gain, ω is a modulation frequency normalized to modulation depth, and δ is a mismatch between the modulation and cavity periods. In the absence of SPM, the

http://dx.doi.org/10.5772/intechopen.70737

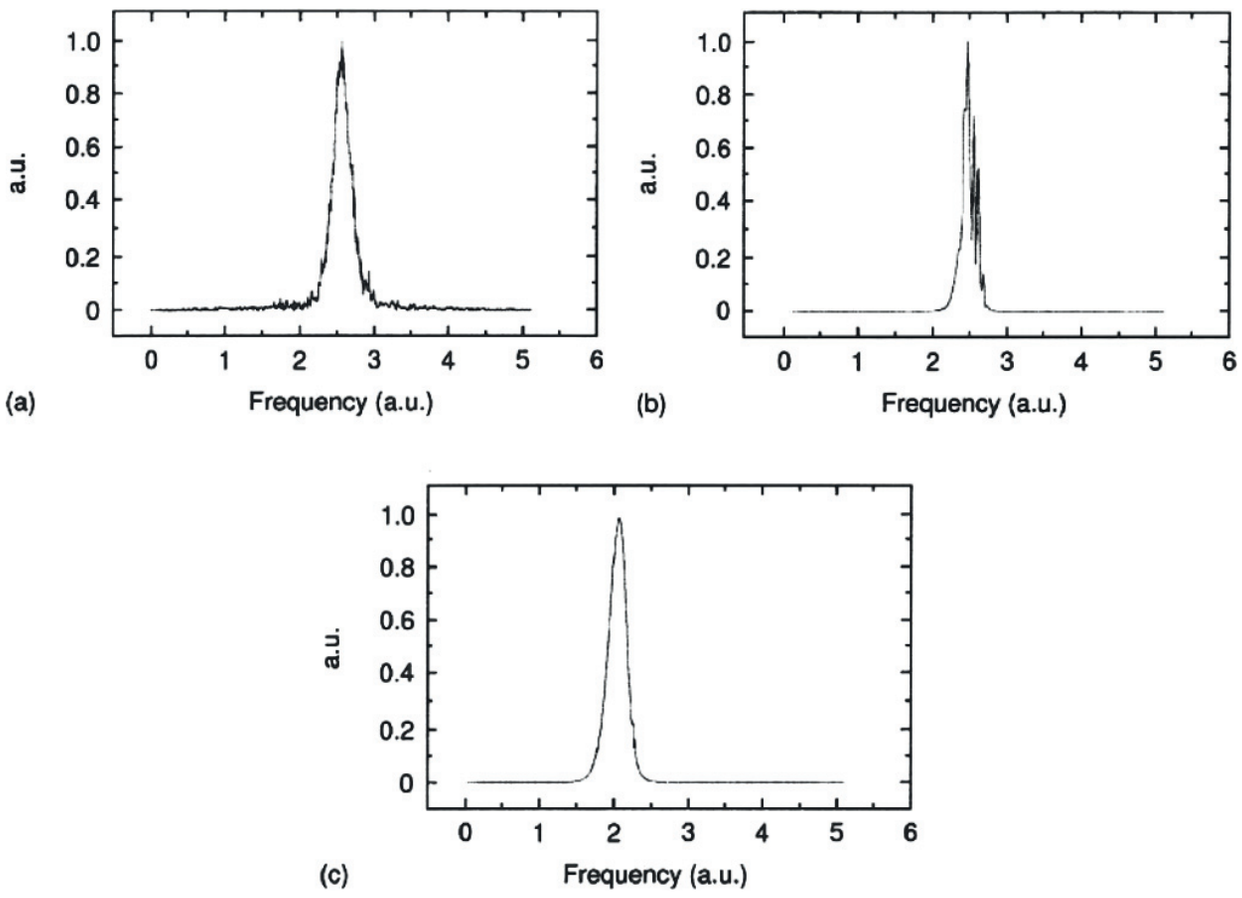

Figure 13. Evolution of noisy pulse with external phase modulation (moving mirror, the modulation frequency is 1 kHz) [53]. (a) Initial noisy pulse; (b) pulse at 1000th cavity transit (noise is sweeping out due to Doppler effect); (c) pulse at 5000th cavity transit (noise is swept out).

pulse width τ is $\tau = 2\sqrt{-\sigma}/|\omega|$. It increases with saturated net-gain $-\sigma$, is closely associated with the modulation frequency ω, and exceeds substantially the minimal value $\sqrt{\alpha}$ defined by spectral dissipation. However, the nonlinearity (namely, SPM) can modify a situation crucially [55, 56]. Firstly, the pulse width decreases (not increases) with a gain that allows generating high energy, and simultaneously, short pulses. Secondly, and it is a first nontrivial fact, pulse width can be extremely short ($\sim 10\sqrt{\alpha}$) and reach scales incommensurable with the modulation frequency. Third impressive fact is that the modulation frequency providing stable mode-locking can be extremely small in comparison with the laser cavity period (ω is lower by approximately three orders of magnitude in comparison with a linear case). It seems that this effect is closely related to the above considered noise suppression due to the Doppler shift.

Returning to an effect of noise on the mode-locking self-start illustrated in **Figure 12**, one may consider another interesting manifestation of SR/SAR in mode-locked lasers. External resonator providing mode-locking can be considered as a Fabry-Pérot interferometer resonantly matched with a laser cavity (see above). This interferometer can contain a nonlinear medium, and such a system possesses rich dynamical properties, in particular, it can cause spontaneous formation of ultra-short pulses (mode-locking). Examples of regions of such mode-locking are

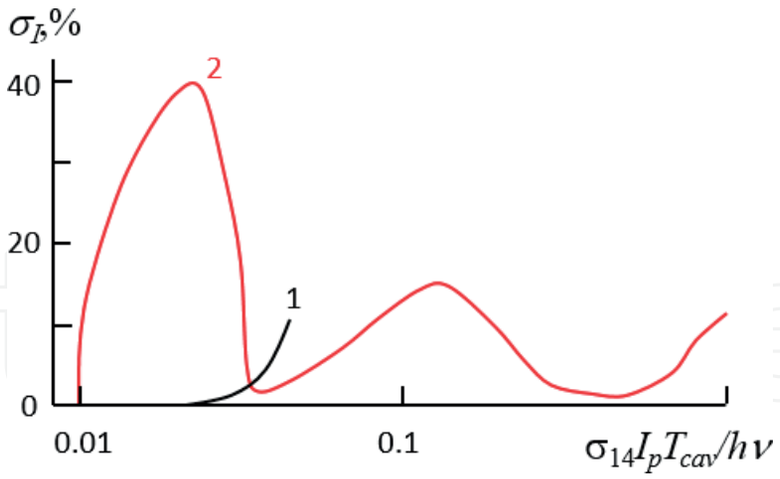

Figure 14. Dependence of mean-square deviation of pulse intensity on the pump in a laser mode-locked by a nonlinear Fabry-Pérot interferometer [53] for the phase mismatch $\varphi = \pi$, reflection coefficients of coupling mirror 0.96 (1), 0.7 (2), and internal transmission of interferometer 0.9 (1), 0.5 (2).

shown in **Figure 12**. It is interesting that such regions are inhomogeneous. **Figure 14** demonstrates the mean-square deviation σ_I of pulse peak intensity inside two such regions in dependence on pump.

One can see, that the pulse is highly stable inside the mode-locking region and destabilizes only on stability border in the case of (1). But in the case of (2), the behavior of σ_I becomes strongly nonmonotonic. Pronounced peaks in the σ_I-dependence is the classical SAR manifestation caused by the excitation of noise with subsequent formation of the pulse satellites whose interaction with main pulse perturbs strongly the latter. The regions of SAR alternate with the regions of regular dynamics. Thus, the mode-locking region can be granulated.

In all examples above considered, a mode-locking resulting in the pulse appearance was caused by either loss self-modulation or external periodical modulation. However, the mode-locking can appear spontaneously due to spontaneous multimode instability (so-called Risken-Nummedal-Graham-Haken effect, RNGH) [57, 58]. However, such self-mode-locking is unstable. Nevertheless, the stable self-mode-locking was obtained in Er-fiber laser due to beatings induced by the difference of intra-laser (fiber + polarization components) birefringence and that induced by polarization hole burning in active medium (Er-doped fiber). That is the so-called *resonance vector mode-locking* [59]. The beatings generate the spectral satellites (sidebands) for each laser mode produced by multimode instability (see **Figure 15**). Adjusting of intra-laser birefringence by polarization controller shifts these sidebands to adjacent modes that cause a resonance between them with subsequent stable mode-locking.

But that is not all. The generated comb of locked modes can excite the transverse acoustic waves in a fiber through electrostriction effect [61]. The resonance between the comb and these waves lock (trap) a pulse in time domain that provides an unprecedented stability of the pulse train. The last is highly required for metrology, high-resolution spectroscopy, etc [62].

http://dx.doi.org/10.5772/intechopen.70737

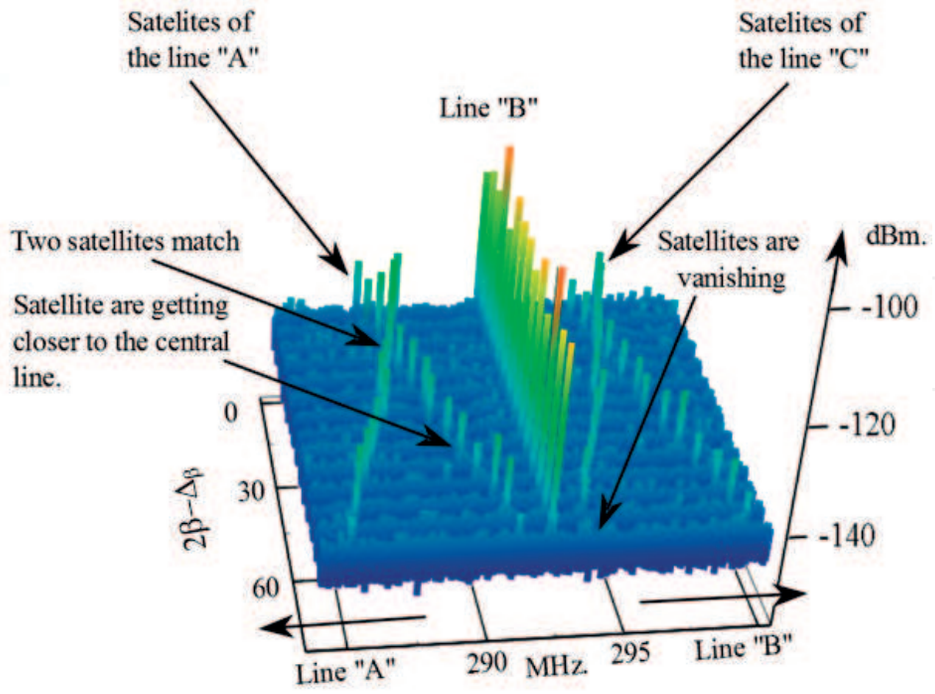

Figure 15. Evolution of spectrum in the vicinity of allocated mode "B" neighboring with modes "A" and "C" [59]. Control parameter is an intra-laser birefringence 2β, Δ_β is a birefringence caused by polarization hole burning in the active fiber [60].

5. Conclusions

The nonlinear resonance phenomena are illustrated as examples of fiber Raman amplifiers and mode-locked lasers. These systems proved their advantage as an ideal test-bed for "metaphoric modeling" of complex nonlinear systems due to comparative simplicity, high-speed statistic gathering, and precise controllability.

We considered the phenomenon of the so-called *stochastic anti-resonance* as examples of a fiber Raman amplifier and a laser mode-locked by resonant coupling with a nonlinear Fabry-Pérot interferometer.

In the first case, the regular polarization beatings between pump and Raman signal are coupled resonantly with the stochastic birefringence caused by material defects (stochastic changes of fiber symmetry). As a result, there is a region of parameters (first of all, so-called polarization mode-dispersion parameter) where the evolution of the state of polarization becomes highly irregular that manifests itself in resonance growth of relative standard deviation of Raman gain. This phenomenon was interpreted as a noise-induced escape from metastable state and quantitatively characterized by an abrupt decrease of the characteristic Kramers length.

In the second case, it is shown a crucial dependence of mode-locking ability on noise correlation time so that the growth of irregularity squeezes the mode-locking region and increases the

mode-locking threshold. Nontrivial effect of noise manifests itself inside the region of parameters, where spontaneously born pulse exists. Namely, a monotonic variation of the pump causes the alternation of maximums and minimums of the pulse peak intensity mean-square deviation. Thus, the stochastic anti-resonances exist inside the mode-locking region, which, thereby, has a granular structure.

The interesting example of *scale hierarchy* in a mode-locked laser is demonstrated. The matter is that extremely slow (~1 kHz), external modulation can suppress noise in mode-locked laser through the Doppler effect. This effect is broadly known for experimenters using the resonator mirror knocking for the mode-locking self-start.

Active mode-locked lasers can demonstrate another aspect of *scale hierarchy* in the nonlinear resonance phenomena. The laser phase nonlinearity coupled with the external phase modulation can provide generation of pulses whose widths are not limited by modulation frequency but only by intra-laser spectral dissipation. Moreover, laser mode-locking can be reached at anomalously low (in comparison with laser resonator round-trip) modulation frequencies. One may bring the last effect into correlation with that mentioned in the previous paragraph, but this issue demands a further consideration.

The phenomenon, which is connected closely with the resonance in systems possessing a scale hierarchy, is a so-called *resonance vector mode-locking*. In this case, a spontaneous locking of laser modes emerging as a result of multimode instability (RNGH) is stabilized due to the polarization beating caused by intra-laser birefringence and birefringence induced by polarization hole burning in the active medium. That results in stable self-mode-locking, which is stabilized additionally through a resonant coupling with the acoustic waves excited by the mode-locking itself through the electrostriction effect.

The *dissipative soliton resonance* with linear waves originating from noise can be considered separately in some way. It is shown, that this resonance defines the dissipative soliton characteristics, namely, its spectral width. When the resonant conditions change due to the contribution of higher-order dispersions (third-order in our case), the dissipative soliton can emit a radiation, which interacts with soliton in turn. As a result, the dissipative soliton dynamics becomes chaotic, that can be classified as *chaotic resonance* in terms of nonlinear resonance of three coupled oscillators.

The unified viewpoint on the nonlinear stochastic and chaotic phenomena in the field of laser physics and solitonics remains undeveloped yet. Such a viewpoint would be a part of general thermodynamic and kinetic theory of dissipative systems promising a strong practical impact in different areas ranging from physics to biology, medicine, and sociology.

Acknowledgements

I acknowledge my colleagues Dr. E. Sorokin and Dr. S. Sergeyev for their valuable contribution to the presented research findings. The author acknowledges the support from Austrian Science Fund (FWF project P24916-N27). Part of computational results has been achieved using the Vienna Scientific Cluster (VSC).

Author details

Vladimir L. Kalashnikov

Address all correspondence to: vladimir.kalashnikov@tuwien.ac.at

Institute of Photonics, Vienna University of Technology, Vienna, Austria

References

[1] Oono Y. The Nonlinear World. Tokyo: Springer; 2013

[2] Scott AC, editor. The Nonlinear Universe. Berlin: Springer; 2010

[3] Lindner B, Garcia-Ojalvo J, Neiman A, Schimansky-Geier L. Effects of noise in excitable systems. Physics Reports. 2004;**392**:321

[4] Benzi R, Parisi G, Sutera A, Vulpiani A. Stochastic resonance in climatic change. Tellus. 1982;**34**:10

[5] Nicolis C. Long-term climatic transitions and stochastic resonance. Journal of Statistical Physics. 1993;**70**:3

[6] Gammaitoni L, Hänggi P, Jung P, Marchensoni F. Stochastic resonance. Reviews of Modern Physics. 1998;**70**:223

[7] Anishchenko VS, Neiman AB, Moss F, Schimansky-Geier L. Stochastic resonance: noise-enhanced order. Physics – Uspekhi. 1999;**42**:7

[8] Wellens T, Shatokhin V, Buchleitner A. Stochastic resonance. Reports on Progress in Physics. 2004;**67**:45

[9] Anishchenko VS, Astakkov V, Neiman A, Vadivasova T, Schimansky-Geier L. Nonlinear Dynamics of Chaotic and Stochastic Systems. Berlin: Springer; 2007

[10] McDonnell MD, Stocks NG, Pearce CEM, Abbott D. Stochastic Resonance: From Superthreshold Stochastic Resonance to Stochastic Signal Quantization. Cambridge: Cambridge University Press; 2008

[11] Andò B, Gaziani S, editors. Stochastic Resonance: Theory and Applications. Dordrecht: Kluwer; 2000

[12] Longtin A. Stochastic resonance in neuron models. Journal of Statistical Physics. 1993;**70**:309

[13] Hänggi P. Stochastic resonance in biology: how noise can enhance detection of weak signals and help improve biological information processing. Chemphyschem. 2002;**3**:285

[14] Lindner B, Schimansky-Geier L, Longtin A. Maximizing spike train coherence or incoherence in the leaky integrate-and-fire model. Physical Review E. 2002;**66**:031916

[15] Moss F, Ward LM, Sannita WG. Stochastic resonance and sensory information processing: a tutorial and review of application. Clinical Neurophysiology. 2004;**115**:267

[16] McDonell MD, Abbott D. What is stochastic resonance? Definitions, misconceptions, debates, and its relevance to biology. PLoS Computational Biology. 2009;**5**:e1000348

[17] McDonell MD, Word LM. The benefits of noise in neural systems: bridging theory and experiment. Nature Reviews/Neuroscience. 2011;**12**:415

[18] Haykin S, Kosko B, editors. Intelligent Signal Processing. New York: IEEE Press; 2001

[19] Benzi R, Sutera A, Vulpiani A. The mechanism of stochastic resonance. Journal of Physics A. 1981;**14**:L453

[20] Benzi R, Sutera A, Vulpiani A. Stochastic resonance in the Landau-Ginzburg equation. Journal of Physics A. 1985;**18**:2239

[21] McNamara B, Wiesenfeld K. Theory of stochastic resonance. Physical Review A. 1989;**39**: 4854

[22] Hänggi P. Escape from a metastable state. Journal of Statistical Physics. 1986;**42**:105

[23] Nikolis G, Nicolis C, McKernan D. Stochastic resonance in chaotic dynamics. Journal of Statistical Physics. 1993;**70**:125

[24] Landa PS, McClintock PVE. Nonlinear systems with fast and slow motions: changes in the probability distribution for fast motions under the influence of slower ones. Physics Reports. 2013;**532**:1

[25] McNamara B, Wiesenfeld K, Roy R. Observation of Stochastic Resonance in a Ring Laser. Physical Review Letters. 1988;**60**:2626

[26] Headley P, Agrawal G, editors. Raman Amplification in Fiber Optical Communication Systems. Amsterdam: Elsevier; 2005

[27] Kalashnikov VL, Sergeyev SV. In: Skiadas C, editor. The Foundations of Chaos Revisited: From Poincaré to Recent Advancements. Switzerland: Springer; 2016. p. 159-179

[28] Lin Q, Agrawal GP. Vector theory of stimulated Raman scattering and its application to fiber-based Raman amplifiers. Journal of the Optical Society of America B: Optical Physics. 2003;**20**:1616

[29] Kalashnikov VLStochastic Anti-Resonance in a Fibre Raman Amplifier "(Commented Matematica/Matlab Code)"https://www.researchgate.net/publication/308233643_Stochastic_Anti-Resonance_in_a_Fibre_Raman_Amplifier

[30] Kalashnikov V, Sergeyev SV, Ania-Castanón JD, Jacobsen G, Popov S. Stochastic phenomena in a fiber Raman amplifier. Annalen der Physik. 2017;**529**:1600238

[31] Kalashnikov V, Sergeyev SV, Jacobsen G, Popov S. Multi-scale polarisation phenomena. Nature Light: Science & Applications. 2016;**5**:e16011

[32] Kramers H. Brownian motion in a field of force and the diffusion model of chemical reactions. Physica. 1940;**7**:284

[33] Akhmediev NN, Ankiewicz A, editors. Dissipative Solitons. Berlin: Springer; 2005

[34] Akhmediev NN, Ankiewicz A, editors. Dissipative Solitons: From Optics to Biology and Medicine. Berlin: Springer; 2008

[35] Sorokin E, Tolstik N, Kalashnikov VL, Sorokina IT. Chaotic chirped-pulse oscillators. Optics Express. 2013;**21**:29567

[36] Telle HR, Steinmeyer G, Dunlop AE, Stenger J, Sutter DH, Keller U. Carrier-envelope offset phase control: A novel concept for absolute optical frequency measurement and ultrashort pulse generation. Applied Physics B: Lasers and Optics. 1999;**69**:327-332

[37] Podivilov E, Kalashnikov VL. Heavily-chirped solitary pulses in the normal dispersion region: New solutions of the cubic-quintic complex Ginzburg-Landau equation. JETP Letters. 2005;**82**:467-471

[38] Kalashnikov VL. In: Al-Khursan AH, editor. Solid-State Laser. Rijeka: InTech; 2012. p. 145-184

[39] Kalashnikov VL, Fernández A, Apolonski A. High-order dispersion in chirped-pulse oscillators. Optics Express. 2008;**16**:4206

[40] Kalashnikov VL. In: Skiadas CH, Dimotikalis I, Skiadas C, editors. Chaos Theory. Modeling, Simulation and Applications. Singapore: World Scientific; 2011. p. 199-206

[41] Baesens C, Guckenheimer J, Kim S, MacKay RS. Three coupled oscillators: mode-locking, global bifurcations and toroidal chaos. Physica D: Nonlinear Phenomena. 1991;**49**:387

[42] Pazó D, Sánchez E, Matías MA. Transition to high-dimensional chaos through quasiperiodic motion. International Journal of Bifurcation and Chaos. 2001;**11**:2683

[43] Abarbanel HDI, Brown R, Sidorowich JJ, Tsimring LS. Practical method for determining the minimum embedding dimension of a scalar time series. Reviews of Modern Physics. 1993;**65**:1331

[44] Kuizenga DJ, Siegman AE. FM and AM mode locking of the homogeneous laser - Part I: Theory. IEEE Journal of Quantum Electronics. 1970;**QE-6**:694

[45] Smith PW. Mode-locking of lasers. Proceedings of the IEEE. 1970;**58**:1342

[46] Kryukov PG, Letokhov VS. Fluctuation mechanism of ultrashort pulse generation by laser with saturable absorber. IEEE Journal of Quantum Electronics. 1972;**QE-8**:766

[47] Glenn WH. The fluctuation model of a passively mode-locked laser. IEEE Journal of Quantum Electronics. 1975;**QE-11**:8

[48] Kalashnikov VL, Kalosha VP, Mikhailov VP, Poloyko IG. Self-mode locking of four-mirror-cavity solid-state lasers by Kerr self-focusing. Journal of the Optical Society of America B: Optical Physics. 1995;**12**:462

[49] Kalashnikov VL, Kalosha VP, Mikhailov VP, Demchuk MI. Self-starting of cw mode-locked solid-state lasers with a linear external cavity. Optics Communications. 1993;**96**: 249

[50] Fleck JA. Ultrashort-Pulse Generation by Q-Switched Lasers. Physics Review. 1970;**B1**:84

[51] Catherall JM, New GHC. Role of spontaneous emission in the dynamics of mode locking by synchronous pumping. IEEE Journal of Quantum Electronics. 1986;**QE-22**:1593

[52] Blow KJ, Wood D. Mode-locked lasers with nonlinear external cavities. Journal of the Optical Society of America. 1988;**5**:629

[53] Kalashnikov VL, Kalosha VP, Mikhailov VP, Poloyko IG. The general approach to mode-locking mechanism analysis for CW solid-state lasers with a nonlinear Fabry-Pérot interferometer. Optical and Quantum Electronics. 1995;**27**:1061

[54] Liu YM, Sun KW, Prucnal PR, Lyon SA. Simple method to start and maintain self-mode-locking of a Ti:sapphire laser. Optics Letters. 1992;**17**:1219

[55] Kalashnikov VL, Poloiko IG, Kalashnikov VP. Generation of ultrashort pulses in lasers with external frequency modulation. Quantum Electronics. 1998;**28**:264

[56] Kalashnikov VL, Poloiko IG, Mikhailov VP. Phase modulation of radiation of solid-state lasers in the presence of Kerr optical nonlinearity. Optics and Spectroscopy. 1998;**84**:104

[57] Risken H, Nummedal K. Self-Pulsing in Lasers. Journal of Applied Physics. 1968;**39**:4662

[58] Lugiato L, Prati F, Brambila M. Nonlinear Optical Systems. Cambridge: Cambridge University Press; 2015

[59] S.A. Kolpakov, S.V. Sergeyev, Y. Loika, N. Tarasov, V. Kalashnikov, G. Agrawal, Resonance vector mode locking. arXiv:1508.05933 [physics.optics]

[60] Sergeyev SV. Fast and slowly evolving vector solitons in mode-locked fibre lasers. Philosophical Transactions of the Royal Society A. 2014;**372**:20140006

[61] Grudinin AB, Gray S. Passive harmonic mode locking in soliton fiber lasers. Journal of the Optical Society of America B: Optical Physics. 1997;**14**:144

[62] Ye J, Cundiff ST. Femtosecond Optical Frequency Comb Technology. Boston: Springer; 2005